JET PRODUCTION AT HERA

J. Spiekermann
Institut für Physik, Universität Dortmund,
44221 Dortmund, Germany

The HERA collider allows the investigation of quasi real γp–scattering as well as deep inelastic ep–scattering. In both kinematic regions jet production can reveal the structure of the colliding particles. Results from two analyses of jet production are presented: the dijet cross sections for direct and resolved processes in photoproduction, the dijet rate in deep inelastic ep–scattering as a function of the photon virtuality Q^2 ($5 < Q^2 < 100$ GeV^2) and as a function of the Bjørken scaling variable x ($10^{-4} < x < 10^{-2}$).

1 Introduction

At HERA, 820 GeV protons and 27.5 GeV positrons collide in the two experiments ZEUS and H1. HERA does not only allow the investigation of deep inelastic ep–scattering at centre of mass energies up to ≈ 300 GeV but is also a facility where collisions of quasi real photons and protons can be studied.

In the experiments these two domains are usually separated by demanding the scattered positron to be or not to be found in the central detector. Both cases can be seen as the collision of a virtual photon $\gamma^{(*)}$ with the proton p.

In both domains events are observed where the hadronic final state contains collimated bunches of particles which are identified by dedicated algorithms as jets. The properties of the jets correspond to those of the partons of the underlying hard process. In the $\gamma^{(*)}p$ centre of mass frame at leading order (LO) two jets with a minimum transverse momentum p_t are produced. The study of dijet events is therefore a natural choice.

In photoproduction, *i.e.* $Q^2 \approx 0$, at LO two kinds of processes contribute to the dijet production which are sketched in figure 1.

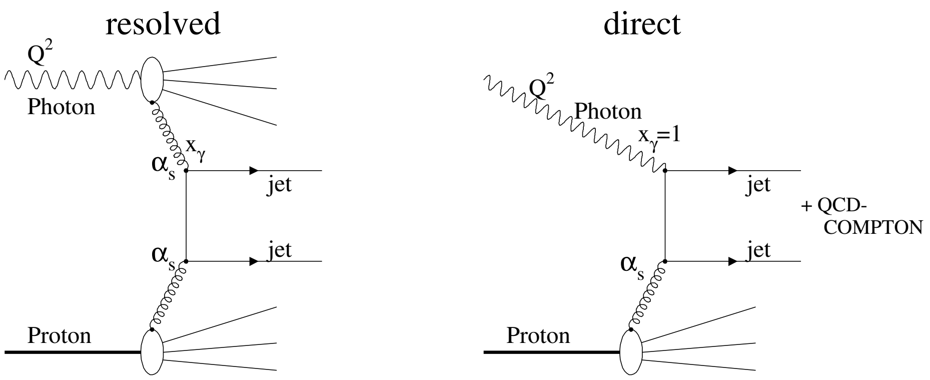

Figure 1:Schematic graphs of leading order processes for dijet production in photoproduction.

In the "resolved" processes the photon first fluctuates into a hadronic state and a parton of the state interacts with a parton of the proton. In "direct" events the photon interacts pointlike with the parton of the proton. The two kinds of processes have clearly distinct characteristics in the final state. The "resolved" processes produce hadronic energy flow in the photon direction whereas the "direct" do not.

In the domain of deep inelastic scattering at high photon virtualities, Q^2, the hard scale in the scattering process is given by Q^2 and only the "direct" processes contribute. However for low Q^2, dijet events with two high p_t jets provide a second hard scale which may be in the same order of magnitude as Q^2 . This is clearly the case for the analysis of deep inelastic scattering events presented in this paper where the transverse momentum, p_t, of the two jets is required to be larger than 5 GeV and the photon virtuality, Q^2, is in the range $5 < Q^2 < 100$ GeV^2. Here it is a priori not clear whether there is a non–negligible contribution from "resolved" virtual photon events or not.

2 Dijet cross section for "direct" and "resolved" events in photoproduction

In non–leading order the distinction between "direct" and "resolved" events as given above is ambiguous. In order to compare measured cross sections with data it is therefore necessary to define "direct" and "resolved" in terms of an observable which is well defined to arbitrary order in theory and in experiment. In this analysis

$$x_\gamma = \frac{\sum_{\rm jets} E_t^{jet} e^{-\eta^{\rm jet}}}{2yE_e} \tag{1}$$

has been used where $E_t^{\rm jet}$ is the transverse energy of each jet and $\eta^{\rm jet}$ the pseudorapidity in the γp rest frame. E_e is the energy of the positron beam and y the inelasticity of the event. x_γ can be interpreted as the fraction of the photon's momentum carried by the parton entering the hard process. In this sense "direct" events are characterized by $x_\gamma = 1$ whereas "resolved" events mostly show x_γ values much smaller than 1. A cut in x_γ distinguishes between "direct" ($x_\gamma > 0.75$) and "resolved" ($x_\gamma < 0.75$) enriched samples.

For the measurement of the dijet cross section as a function of the mean pseudorapidity $\bar\eta$ the following event selection has been applied: no scattered positron in the central detector which means $Q^2 < 4$ GeV^2 where $\langle Q^2\rangle \approx 10^{-3}$ GeV^2, $0.2 < y < 0.8$ which corresponds to $134 < W_{\gamma p} < 269$ GeV where $W_{\gamma p}$ is the centre of mass energy of the γp system, at least two jets with transverse energy $E_t^{\rm jet} > E_t^{\rm min}$ for values of $E_t^{\rm min}$=6, 8, 11 or 15 GeV which have pseudorapidities $-1.375 < \eta^{\rm jet} < 1.875$ and $|\Delta\eta^{\rm jet}| < 0.5$. The jet identification has been performed with the KTCLUS jet algorithm [1,2)]

Figure 2 shows the differential dijet cross section $d\sigma/d\bar\eta$ in comparison with a next to leading order (NLO) calculation [3)]. For the "direct" events ($x_\gamma > 0.75$) the measured cross section is reasonably well described by the NLO calculation for all values of $E_t^{\rm min}$.

The measurement of the cross section for "resolved" events has been restricted to the range $0.3 < x_\gamma$. Below this value the observed cross section is not described by the HERWIG generator which has been used for the correction of the data.

The comparison to the NLO calculation shows large discrepancies between data and calculation. The discrepancies are largest for low values of $E_t^{\rm min}$ and seem to decrease with increasing $E_t^{\rm min}$. In "resolved" events the photon and proton remnant may interact in addition to the hard process which leads to additional energy flow in the hadronic final state. Therefore the measured transversal energy of the jets is biased. The effect is largest for lowest $E_t^{\rm jet}$.

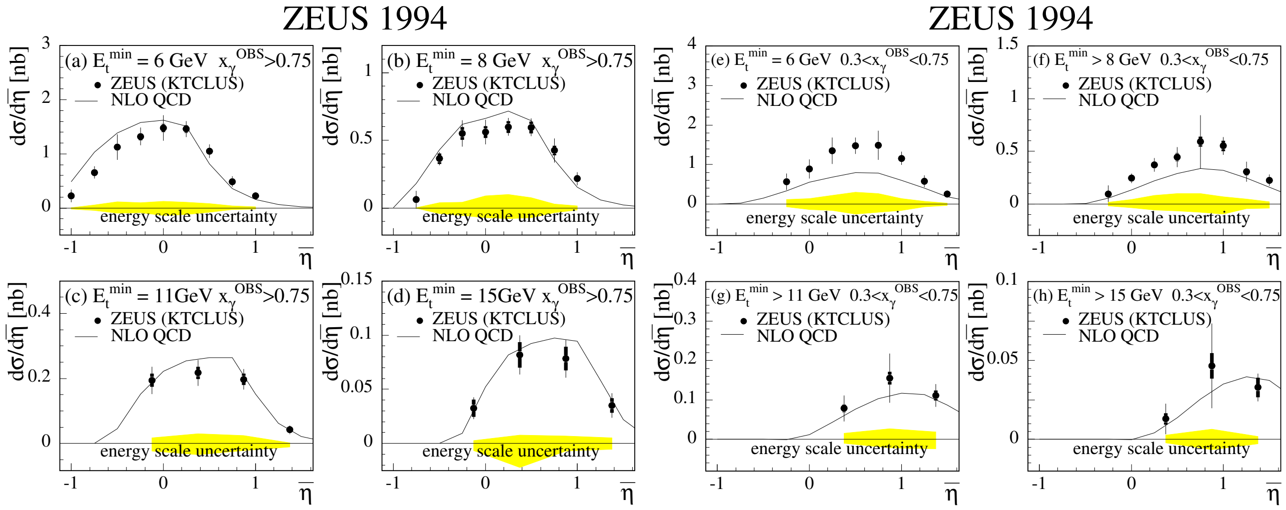

Figure 2:Dijet cross section $d\sigma/d\bar{\eta}$ as a function of the mean pseudorapidity $\bar{\eta}$ of the two jets for different minimum values of $E_t^{\rm jet}$. The $\bullet$ denote the data with statistical (inner bars) and full error. The shaded band indicates the additional uncertainty from the energy scale of the calorimeter. The full line shows a NLO prediction by Kramer and Klasen [3]. Figures (a) to (d) represent the "direct" events and figures (e) to (h) the "resolved".

3 Dijet rates in deep inelastic scattering

The domain of deep inelastic scattering is experimentally defined by demanding the scattered positron to be found in the central detector. This corresponds roughly to a minimum value for Q^2 of 5 GeV^2. In this domain the dijet rate $\mathcal{R}_2$, *i.e.* the ratio of the dijet cross section and the total cross section, has been measured as a function of either Q^2 or x. Hereby the events fulfill the following selection requirements: the scattering angle, θ_e, of the scattered positron is in the range $156° < \theta_e < 173°$, the positron energy, E_e, is $E_e > 11$ GeV and the inelasticity, y, of the event is $y > 0.05$. Dijet events are selected by the additional cuts on the hadronic final state: two jets with a transversal momentum $p_t > 5$ GeV and $|\Delta\eta| < 2$ where $\Delta\eta$ is the difference of the pseudorapidities of the two jets. All jet quantities are evaluated in the $\gamma^* p$ rest frame and the jets are identified by a cone algorithm [4] with a cone radius of 1.0.

Figure 3 shows the dijet rate as a function of either Q^2 or x in comparison to several predictions. In principle standard Monte Carlo generators like LEPTO [5] should describe the properties of deep inelastic scattering events. LEPTO uses the leading order matrix element for dijet production and includes higher orders effects by DGLAP based parton showers. However, it turns out that LEPTO is not at all able to describe the dijet rate especially for low values of Q^2 or x. This may be due to the only approximative inclusion of higher order effects through parton showers. Therefore the dijet rate has also been determined with NLO matrix element calculations using the program DISENT [6].

Matrix element calculations do not include the hadronization step. Therefore, to compare the results to the measured dijet rate hadronization corrections have to be taken into account. Studies with LEPTO and ARIADNE gave hadronization corrections below 25% in the investi-

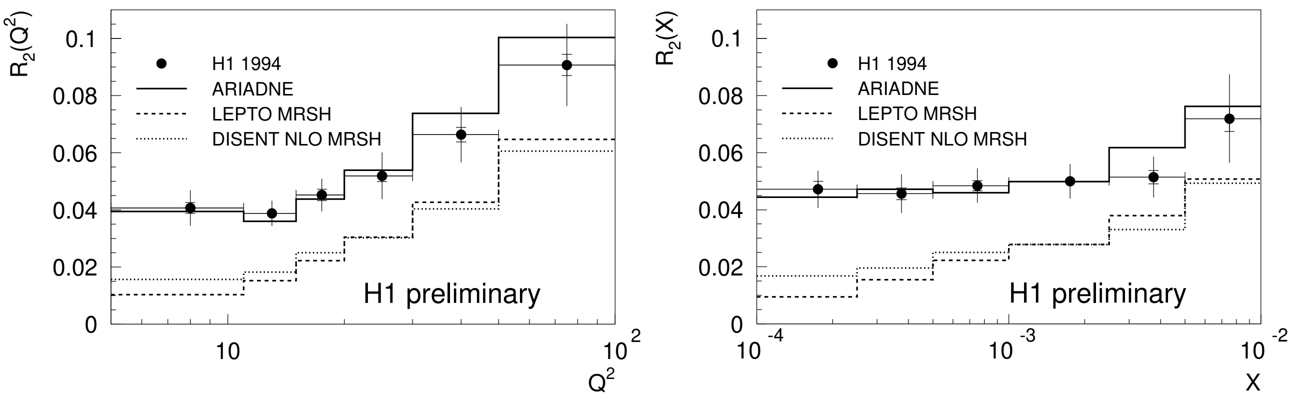

Figure 3:Dijet rate $\mathcal{R}_2$ in deep inelastic ep scattering as a function of Q^2 (left) and x (right). The • denote data with statistical (inner bars) and full error. The lines show predictions form different models.

gated kinematic region. Considering this, figure 3 shows that the prediction of DISENT agrees reasonably well with the LEPTO prediction and therefore reveals the same large discrepancies to the measured dijet rate.

The ARIADNE Monte Carlo [7)] describes the observed dijet rates perfectly well, the absolute height as well as the functional dependence on Q^2 or x. Unfortunately the ARIADNE Monte Carlo relies on some phenomenological ideas. Therefore hard conclusions are difficult. However, it should be noted that ARIADNE contains in a simple approach a contribution from "resolved" virtual photon events which neither LEPTO nor the matrix element calculations do.

To clarify whether there is a contribution from "resolved" virtual photon events or not one can exploit characteristics of the hadronic final state as mentioned in section 1. A hadronic energy flow in the photon direction causes a reduced value of x_γ. The higher the contribution of "resolved" events is the more events should have low x_γ values. Furthermore the fraction of "resolved" events should decrease with the virtuality of the photon. Consequently the x_γ distribution should show a dependence on Q^2 in case of a substantial contribution of "resolved" events.

Figure 4a shows the x_γ distribution in three different bins in Q^2 for measured dijet events. The distribution is normalized to the number of events. An increase of the number of events having low x_γ values with decreasing Q^2 is clearly observed as it is expected for a contribution from "resolved"events. Due to the normalization of the histogram this is accompanied by a decrease of events at high x_γ values.

However, since this distribution is shown for uncorrected data it is not clear whether this rise is due to detector effects. This is shown not to be the case by an investigation of events generated by the LEPTO generator which does not produce a "resolved" contribution. Figure 4b shows the x_γ distribution for these events where the full detector response has been simulated. No significant changes in the x_γ distribution for the different Q^2 bins are observed.

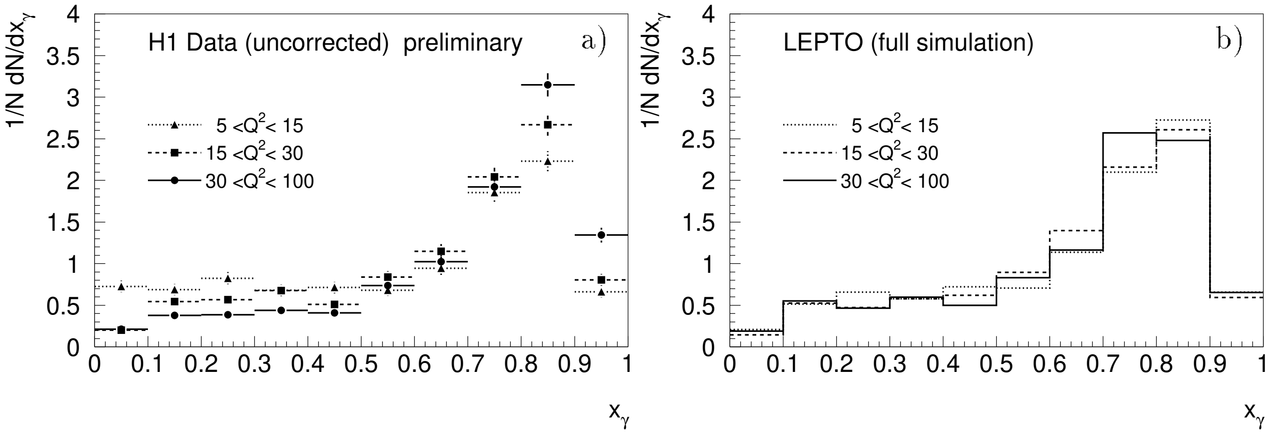

Figure 4:The measured x_γ distribution in three different bins in Q^2 for measured dijet events (a) and simulated events of LEPTO (b).

Thus the dependence of the measured x_γ distribution on Q^2 has to be interpreted as an indication for a non–negligible contribution of "resolved" events to the dijet rate at low values of Q^2.

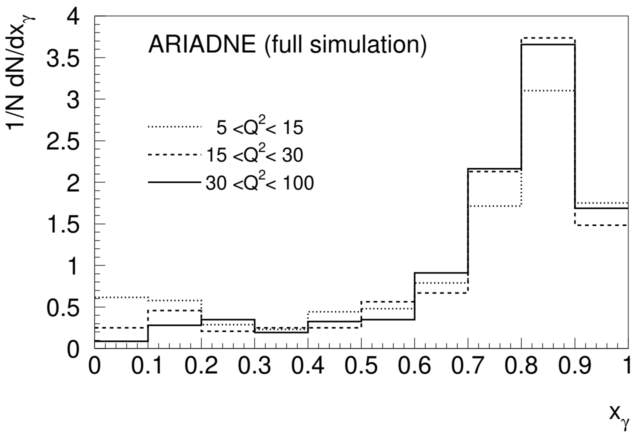

Figure 5:The x_γ distribution for simulated events of ARIADNE in three different bins in Q^2.

Since the ARIADNE Monte Carlo program describes perfectly the observed dijet rates it is interesting to see whether it renders the x_γ distribution and its behaviour with Q^2 as well.

Figure 5 shows the x_γ distribution for fully simulated events which have been generated by the ARIADNE Monte Carlo program. Although it is not able to describe the measured x_γ distribution in all details it nevertheless shows a similar dependence on Q^2.

References

(1) S. Catani, Yu.L. Dokshitzer, M.H. Seymour and B.R. Webber, Nucl. Phys. B406 (1993)
(2) S.D. Ellis, D.E. Soper, Phys. Rev. Lett. 69 (1993) 3615
(3) J.M. Butterworth, L. Feld, M. Klasen, G. Kramer, in Proc. "Future Physics at HERA" (DESY Hamburg) 1995/96, hep-ph/9608481
(4) CDF Collaboration, F. Abe et. al. Phys. Rev. D 45 (1992) 72
(5) G. Ingelman, A. Edin, J. Rathsman, Comp. Phys. Comm. 101 (1997) 108
(6) S. Catani, M.H. Seymour, Nucl. Phys. B 485 (1997) 291, hep-ph/9605323
(7) B. Andersson, G. Gustafson, L. Lönnblad, U. Petterson, Z. Phys. C 43 (1989) 625 and references therein